# METHODS OF ESTIMATING FORCES IN BURIED ARCHES

by

MOUNIR G. EL-AASAR

B.S., Alexandria University,
Alexandria, Egypt,
1983

- - - - - - - - - - - - - - - - - - - - - -

A MASTER'S REPORT

submitted in partial fulfillment of the

requirements for the degree

MASTER OF SCIENCE

Department of Civil Engineering

KANSAS STATE UNIVERSITY
Manhattan, Kansas

1988

Approved by:

Wayne W. Williams
Major Professor

TABLE OF CONTENTS

## INTRODUCTION

Higher fills, complicated interchanges, and wider pavements have made drainage requirements increasingly critical. Highway culverts must be larger and in some instances structurally heavier than was customary in the past. They can no longer be considered minor structures.

Arch conduits are of great advantage where hydraulic efficiency is important and they are satisfactory for a wide range of load conditions, being particularly economical under high fills where a relatively thin section has great strength because of the shell or arch action.

The construction of arch conduits has the disadvantage of requiring somewhat more difficult formwork than the box structure. However, this problem does not exist anymore since the invention of the inflated forms in 1985 (3) when the construction of arch conduits became even more economic and efficient.

These inflated forms are cylindrical, closed-ended air bags. They can be inflated; then reinforcement steel and concrete are placed on the outside of the balloon according to the requirements of the design. Later on, the inflated form can be deflated and reused in another place.

Economical design of highway culverts also requires proper attention to structural details, where the conduit can support the embankments and the wheel loads safely.

## PURPOSE OF THE REPORT

The purpose of this report is to present practical suggestions for the structural design of buried arches. In this report, a review of the different methods of calculating the loads on buried arches and the internal forces in the arch members are presented. Also, comparison between results obtained from different methods and the finite element method will be presented. Also in this report, approximate equations to use the finite element method will be presented. The author will also introduce the calculations for two cases of buried arches, using the virtual work method for the purpose of comparison.

Hopefully, this report will be of value to practicing geotechnical engineers in estimating the loads on buried arches due to embankments and wheel loads and also in estimating the forces in the arch members for the purpose of design.

## 1. LOADS ON BURIED ARCHES

Buried arches such as in culverts and conduits must be designed to support the weight of the embankment and the wheel loads of highway, airport, or railway traffic safely and economically. This requires consideration of embankment height, type and strength of pavement, and expected traffic loads.

In designing conduit for live loads, it is necessary first to determine how significant the live load effect is. Rigid pavements distribute traffic loads widely over subgrade areas; consequently, little live load is transmitted from the pavement surface to the buried arch. Significant live loads are transmitted through flexible pavements or where there is no pavement. However, the live load diminishes rapidly as the depth of cover over the arch increases, and highway traffic loads may be disregarded when fill heights exceed 10 ft. (5).

### 1.1 Embankment Vertical Loads on Buried Arches

The intensity of pressure transmitted from embankment materials to a buried arch depends on the depth of backfill and its soil characteristics. The variable factors that represent soil characteristics are angle of internal friction, density, homogeneity of material, and percent of contained moisture (8). The designer should choose the combination of soil characteristics likely to occur during the life of the arch that would subject the structure to the greatest possible stress.

According to the Marston Theory (7), developed by Anson Marston, for estimating the embankment loads on buried arches, the resultant vertical load produced by an embankment is considered to be made up of two parts:

(i) The weight of the column of fill directly over the arch, which has a minimum depth at the crown and a maximum depth at the springing. For deep fills, the column may be considered uniform in length.

(ii) The friction forces acting either upward or downward on the sides of this column of fill. For shallow fills where the height does not exceed the horizontal span of the arch, the friction forces can safely be ignored (5). For higher fills, they should be included in the load determination since they may increase or decrease the load on the culvert.

The settlement of the fill adjacent to the conduit relative to the fill directly over the conduit determines the magnitude and direction of friction factors for a given installation (4).

(a) A greater settlement in the fill material adjacent to the arch--due to compressible subsoils, insufficient compaction of the fill, or simply a greater height of material adjacent to the arch than over it--will set up friction factors acting downward on the fill above the arch, called "negative arching" (Fig. 1). When that happens, the resultant load on the conduit is greater than the weight of the material above it.

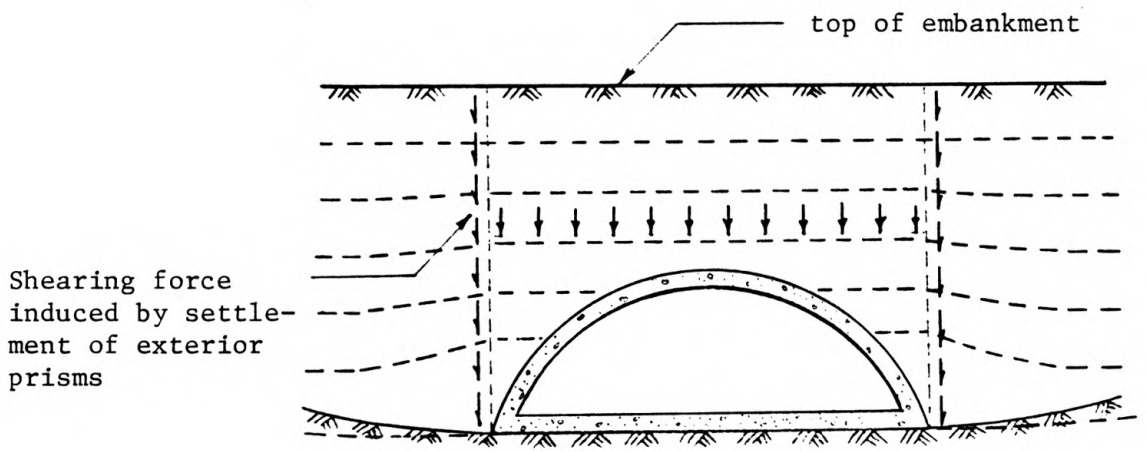


Friction factors increase embankment load on a culvert as the embankment settles downward relative to the fill over the arch.

Fig. 1. Friction forces, unyielding foundation.

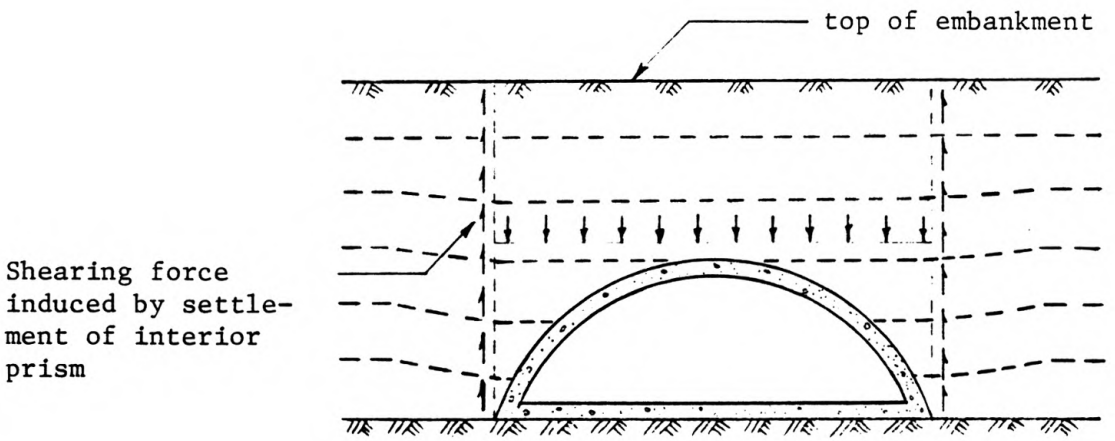


Friction factors decrease embankment load on the culvert as the fill over the arch settles downward relative to the adjacent embankment.

Fig. 2. Friction forces, yielding foundation.

(b) If the settlement is greater directly above the conduit, or if the conduit settles slightly into its foundation, the load is reduced by the amount of the friction forces, which then act upward, called "positive arching" (Fig. 2).

When there is no differential settlement between the fill adjacent to the arch and the fill over it, the resultant load is, of course, equal to the weight of the fill material directly over the arch.

**Calculating Earth Loads on Buried Arches**

The 1969 AASHTO Specifications, Section 1.2.2(A), recommend that the earth loads on buried arches be computed as the weight of the earth directly above the structure.

In computing the total load on an arch, two conditions are considered (5):

(i) Arch in a trench on an unyielding subgrade, or culvert untrenched on a yielding foundation (Fig. 3 a & b):

$$W = PB_c = wHB_c. \qquad (1)$$

(ii) Arch untrenched on an unyielding foundation (such as rock or piles) (Fig. 3.c):

$$W = PB_c = wB_c\ (1.92\ H - 0.87\ B_c) \text{ for } H > 1.7\ B_c, \qquad (2)$$

or

$$W = PB_c = 2.59\ wB_c^2\ (e^K - 1) \quad \text{for } H < 1.7\ B_c, \qquad (3)$$

where: $W$ = total load in pounds per linear foot of arch due to earth backfill,

$P$ = unit load in psf due to earth backfill,

$B_c$ = external horizontal span for arches under embankments or trench width at top of arch for culverts in trenches,

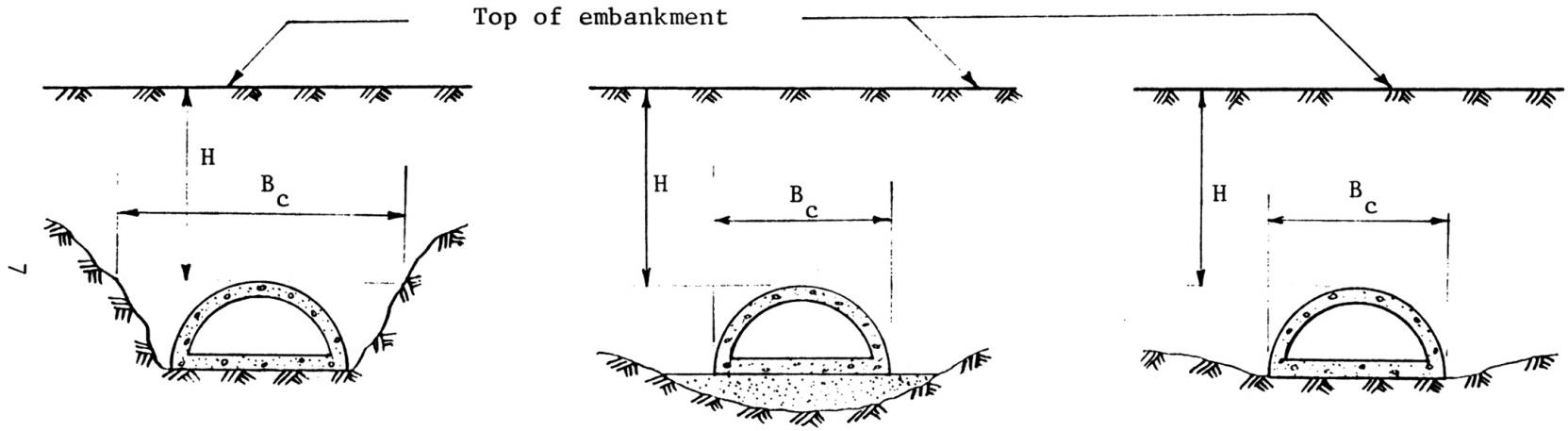


(a) Trench (b) Yielding Foundation (c) Unyielding Foundation

Fig. 3. Different conditions considered in computing the total load on an arch.

w = effective weight of fill material in pcf, which may be taken as 70% of actual weight,

e = base of natural logarithms = 2.7183,

$K = 0.385 \frac{H}{B_c}$, and

H = height of fill in feet over the crown of the arch.

Figures 4, 5, and 6 give total vertical earth loads for arches of various spans and for various fill heights.

Figure 4 is for arches in trenches or for arches on a yielding foundation. Figures 5 and 6 are for culverts on unyielding foundations.

The vertical load obtained from the equations or the charts is always assumed to be distributed uniformly over the top of the arch.

### 1.2 Embankment Lateral Loads on Buried Arches

In general, lateral loads counteract and reduce stresses due to vertical loads. Consequently, ignoring them provides an additional safety factor in the design.

Lateral loads in embankments are of two types, active and passive. Active loads result from the action of the embankment in attempting to assume its natural slope or angle of repose. Active lateral loads are a direct function of vertical loads and may be estimated with fair accuracy, particularly if the soil density and coefficient of internal friction are known. Passive loads are induced by the movement of a structure against the supporting material. Its magnitude is a function of the amount of movement and of the soil characteristics (1, 6).

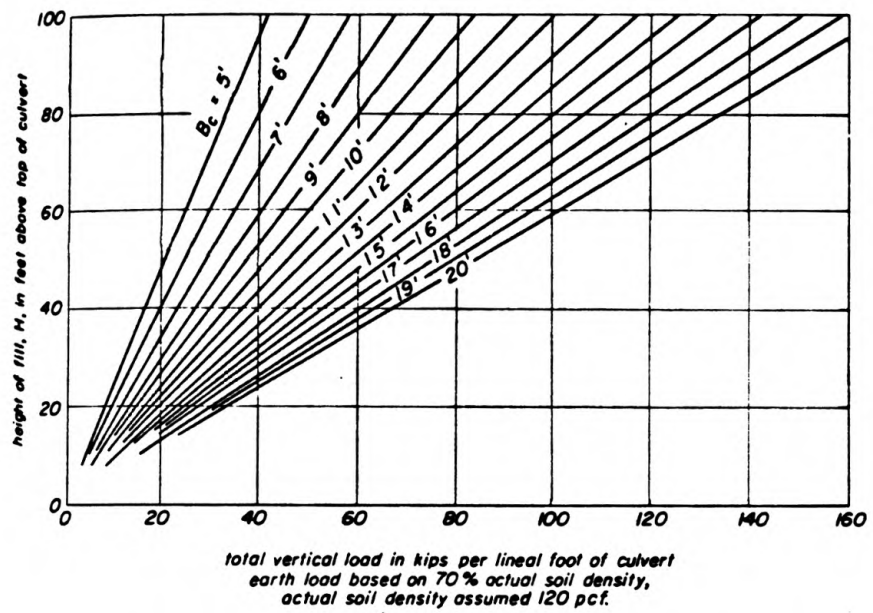


Fig. 4. Total earth load, trench condition or yielding foundation.

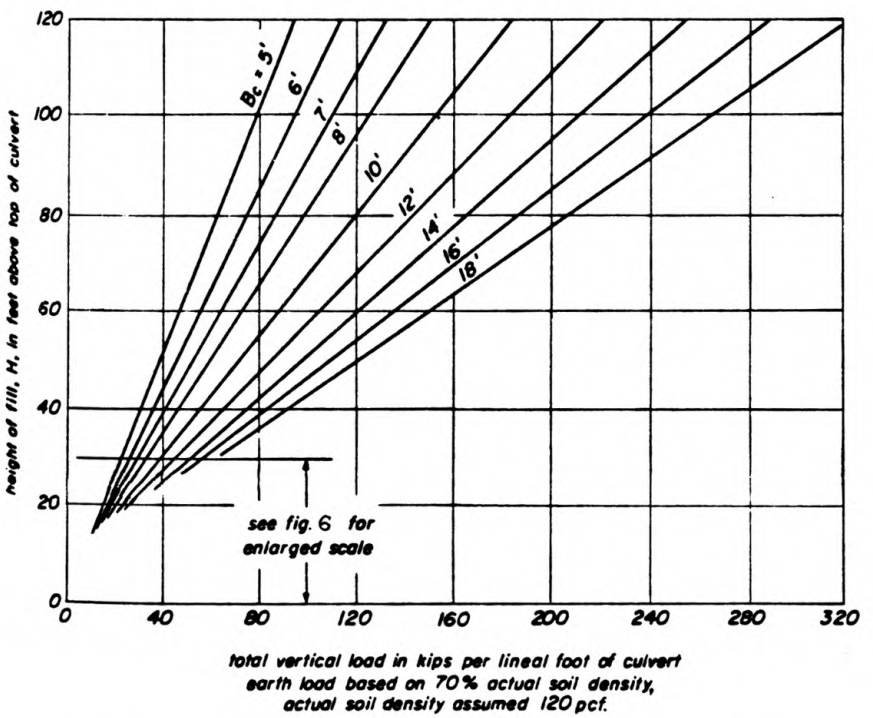


Fig. 5. Total earth load, unyielding foundation.

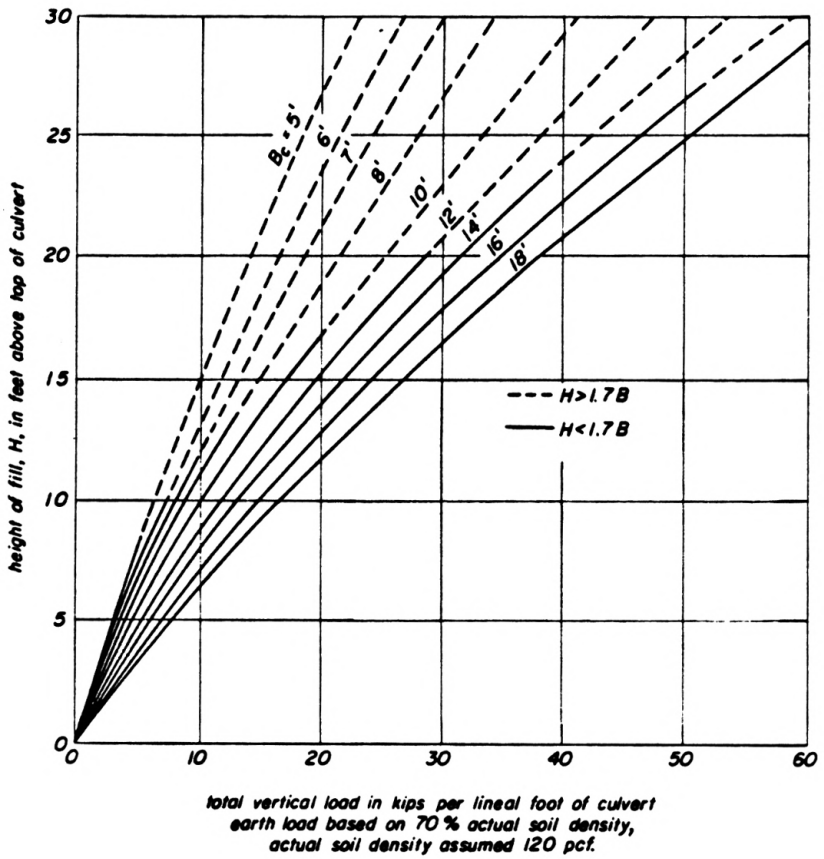


Fig. 6. Enlarged portion of Fig. 5.

By Rankine's Theory, the intensity of active lateral load is K times the intensity of vertical load,

$$K = \frac{1 - \sin \emptyset}{1 + \sin \emptyset} ,$$

where $\emptyset$ = the angle of repose.

The angle of repose for the average fill material used in embankments may be assumed to be $30^{o}$; then K = 0.333, and the intensity of active lateral load at a point in an embankment then is equal to one-third the intensity of vertical load at that point.

In the case of arch conduits built above the natural ground, the embankment is alongside and over it. An excellent compaction of the fill material adjacent to the arch will cause full development of active lateral load.

The practice usually followed in designing arch conduits is to assume the vertical load uniformly distributed over the horizontal projection of the curved surface. Similarly, the active lateral load is assumed to act on the vertical projection of the curved surface (Fig. 7.a).

It may be sufficiently accurate to assume the average lateral load to be acting uniformly over the vertical projection (12), particularly when the height of the structure is low relative to the depth of fill over it (Fig. 7.b).

Embankment conditions change through the lifetime of the arch. Embankments can become saturated, and different intensities of vertical and lateral load may occur. Designs are customarily based

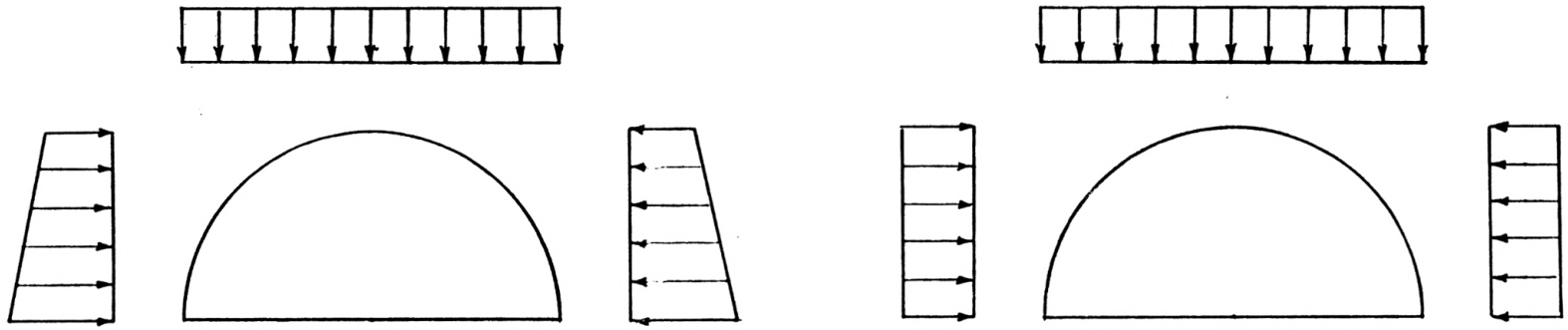

(a) Trapezoidal lateral earth pressure.

(b) Uniform lateral earth pressure.

Fig. 7. Earth Pressure on Arches.

on the maximum vertical loads and minimum lateral loads that may be expected to occur.

### 1.3 Highway Live Loads on Buried Arches

The maximum live load on arch conduits is that produced by heavy trucks. Figures 8 and 9 show the standard truck loadings (H- and HS-loadings) and Fig. 10 the lane standard loadings used by the American Association of State Highway and Transportation Officials (AASHTO) (5).

The H-loadings consist of a two-axle truck (Fig. 8), or the corresponding lane loading (Fig. 10). These loadings are designated by H followed by a number which represents the gross truck weight in tons.

The HS-loadings consist of a tractor truck with a semi-trailer (Fig. 9) or the corresponding lane loading (Fig. 10). These loadings are designated by HS followed by a number which represents the gross truck weight in tons.

The magnitude of the traffic load transmitted to an arch conduit through an earth fill depends on the magnitude of the wheel load, the depth of fill, and the type of pavement.

Rigid pavements distribute traffic loads over large subgrade areas, with consequent low pressure intensity, while flexible pavements do not provide the live load distribution effect typical of rigid pavements. Therefore the analysis of live loads where there is no pavement can be assumed to apply to flexible pavements also.

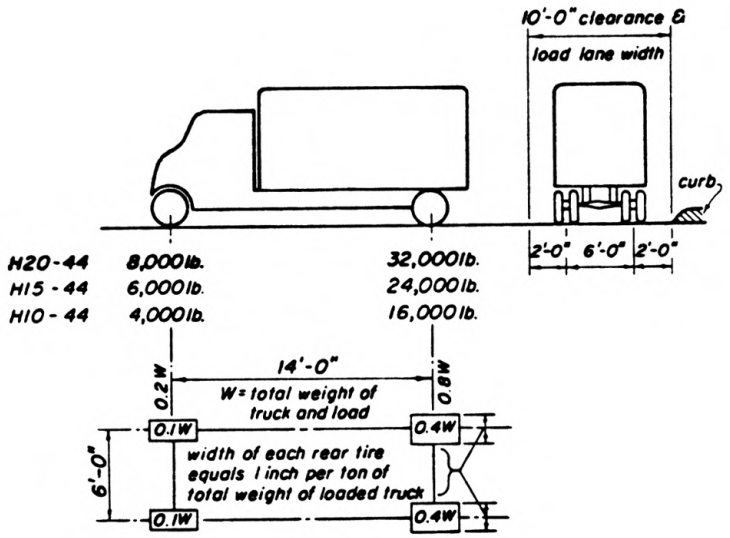


Fig. 8. AASHTO standard truck loadings.

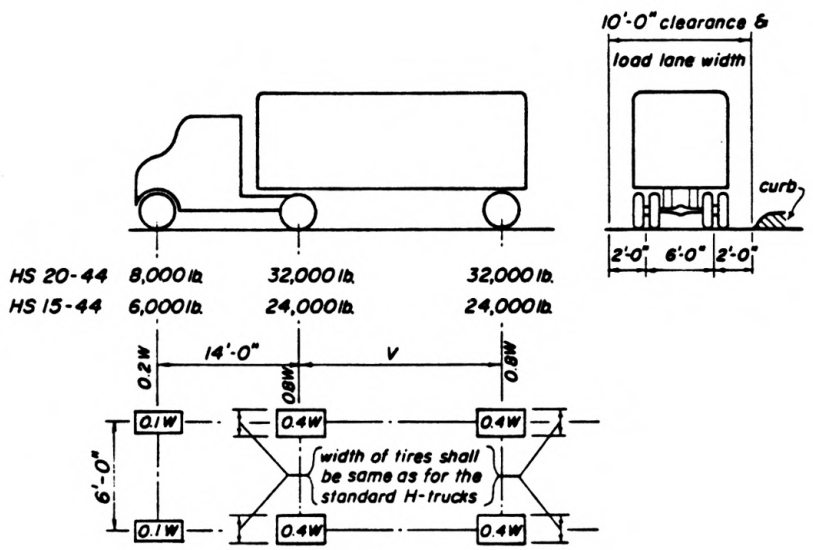


W = combined weight on the first two axles which is the same as for the corresponding H-truck

V = variable spacing - 14 ft. to 30 ft. inclusive. spacing to be used is that which produces maximum stresses.

Fig. 9. AASHTO standard semi-trailer loadings.

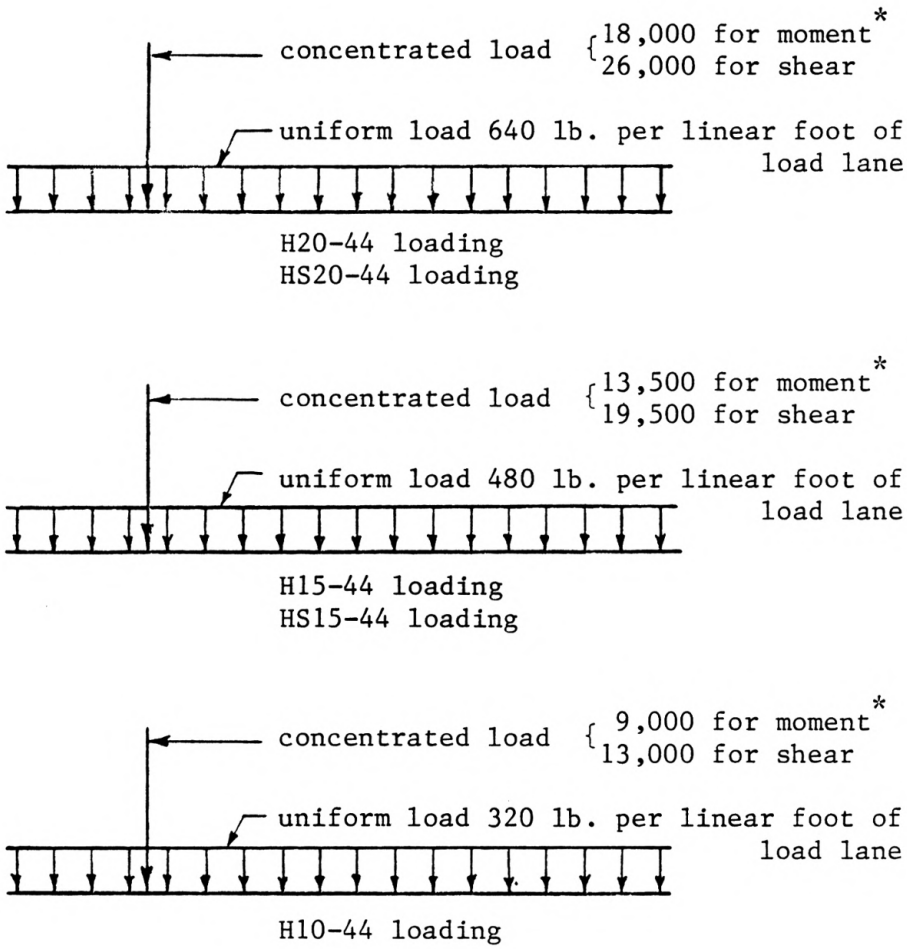


*for continuous spans another concentrated load of equal weight should be placed in one other span in such a position as to produce maximum negative moment.

Fig. 10. AASHTO standard lane loadings.

### 1.3.1 AASHTO Wheel Load Distribution

a. When the depth of fill is less than 2 ft., AASHTO specifies that the wheel load be distributed as on an exposed slab (no fill).

b. When the depth of fill is 2 ft. or more, concentrated loads are to be uniformly distributed over a square, the sides of which are equal to 1.75 times the depth of fill.

c. When the areas from several concentrations overlap, the total load is considered uniformly distributed over the area defined by the outside limits of the individual areas (see Fig. 11).

According to the AASHTO wheel load distribution, the uniform load per lineal foot of arch conduit at the top of the culvert can be determined from the curves of Fig. 12. It will be noted that the loading decreases as the depth, H, increases. The loading also increases as the span increases until the span equals 1.75H. For spans in excess of 1.75H, the loading is constant and acts over only a part of the span.

The loading represented by these curves must be increased to include the effect of impact according to the following impact factors ("Standard Specifications for Highway Bridges," AASHTO, 1969):

| | |
|---|---|
| Cover 0 to 1 ft.-0 in. | I = 1.30 |
| Cover 1 ft.-1 in. to 2 ft.-0 in. | I = 1.20 |

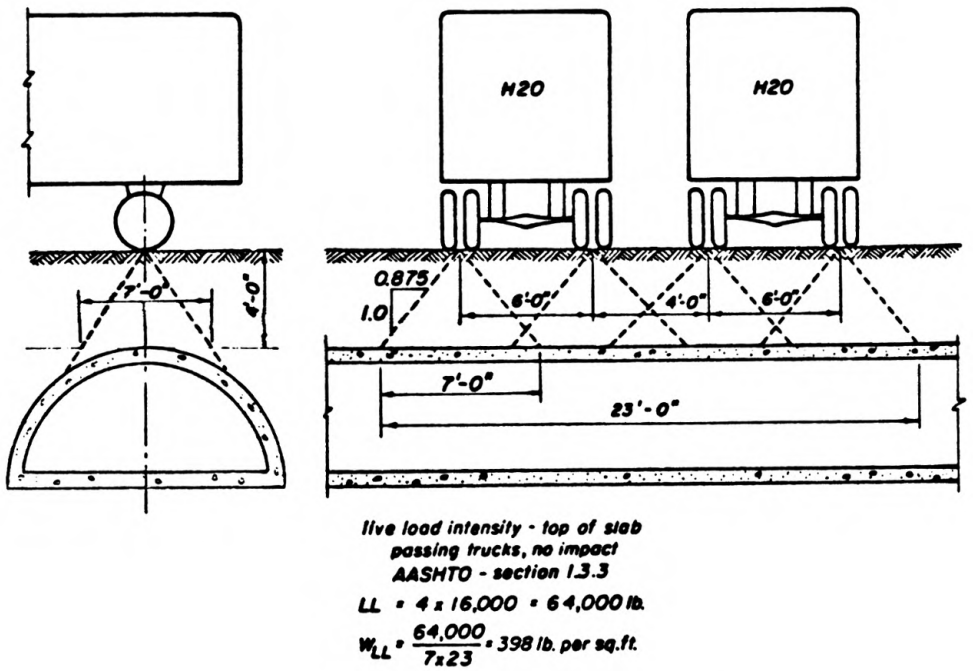


Fig. 11. Live load distribution, adjacent lanes.

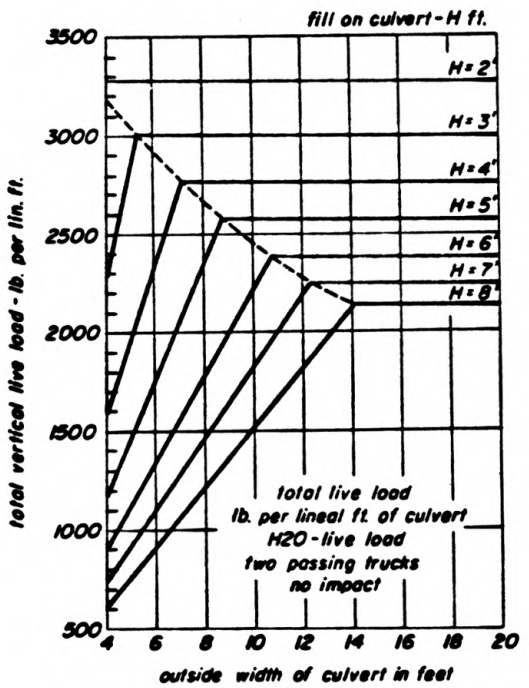


Fig. 12. Total live load on culvert, various widths and fill depths.

Cover 2 ft.-1 in. to 3 ft.-0 in. I = 1.10

Cover over 3 ft.-0 in. I = 1.00

The curves in Fig. 12 are for H20 truck wheel loads. The loadings due to other wheel loads are directly proportional; i.e., loadings due to an H10 truck are exactly half of those given by the H20 curves.

### 1.3.1.a Theoretical Distribution of Wheel Loads on Subgrade or on Flexible Pavement

Subsurface pressures on top of the arch conduit are calculated from the tire pressure, the individual wheel loading, the depth of cover, and the lateral offset from the center of the wheel load to the point in question.

The first step is to determine the area of tire contact with the ground surface. It is satisfactory to consider this area of contact to be a circle. The radius is determined from the following formula (5),

$$a = \sqrt{\frac{W}{\pi P_o}}$$

where

a = radius of the circular contact area, in.

W = load applied by a single wheel, lb.

$P_o$ = tire pressure, psi.

$\pi$ = 3.14

The vertical pressure P on any point on the conduit is

$P = CP_o$

where C is a coefficient which depends on the radius of circular contact area a in inches, and Y the depth of soil between the tire and the top of the conduit and X the horizontal distance between the center line of the tire and the point of question (Fig. 13).

### 1.3.1.b Theoretical Distribution of Wheel Loads on Rigid Pavement

A similar procedure is used to calculate subsurface pressures for wheel loads applied to rigid pavement slabs. In place of the radius of the tire contact area, the radius of stiffness of the pavement slab is used.

This radius of stiffness can be calculated from the formula (5),

$$L = \sqrt[4]{\frac{Eh^3}{12\ (1-\mu^2)K}},$$

where

L = radius of stiffness of slab, in.,

E = modulus of elasticity of concrete, psi.,

h = thickness of concrete slab, in.,

$\mu$ = Poisson's ratio for concrete, assumed constant and equal to 0.15, and

K = modulus of subgrade reaction, assumed constant, pci.

The vertical pressure P on any point on the conduit is

$$P = C\,\frac{W}{L^2},$$

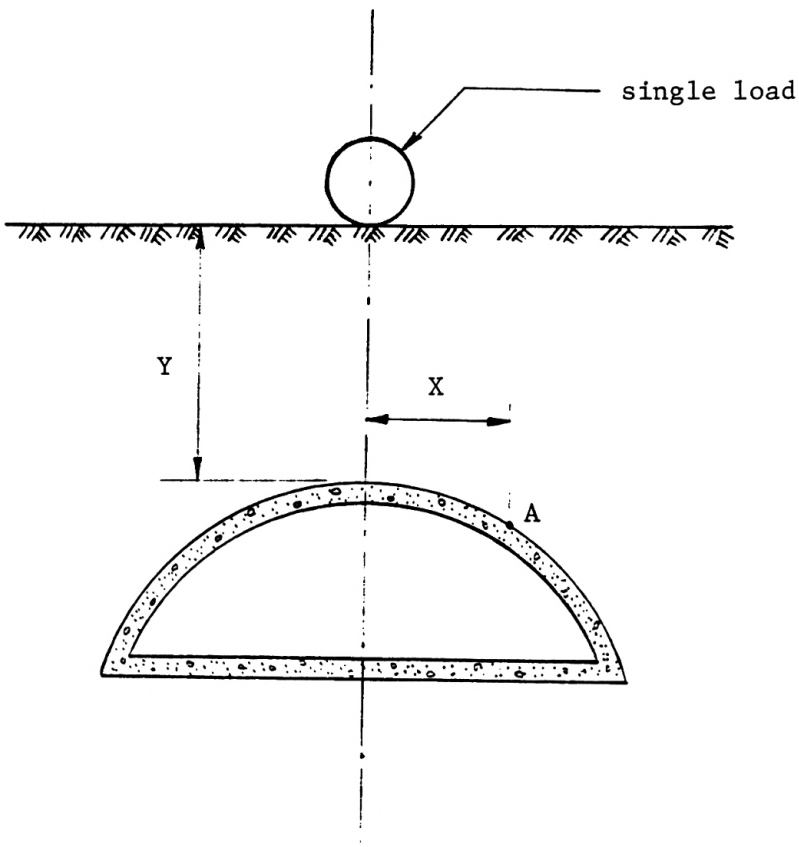


Fig. 13. Y and X for calculating the vertical unit pressure on any point A on the conduit.

where C is a coefficient which depends on the radius of stiffness of slab, Y, and X (Fig. 13).

## 2. FORCES IN BURIED ARCHES

For the design of buried arches, thrust and bending moment must be checked to evaluate the safety of the structure. Also, the behaviour of the footing is important. The footing can experience large downward punching deflections with respect to the floor slab, and if the floor slab is integral with the arch, large moments can be developed near the springings (4).

To carry out the design of an arch conduit, the engineer must account for two equally significant stages (9):

(1) During construction, the conduit must be stiff enough to support its own weight, to maintain its shape, and to permit satisfactory construction of the surrounding embankment.

(2) During service, the soil-structure system must be able to carry the applied dead, thermal, and live loadings, and the conduit wall must accept its share of these loads with an adequate factor of safety against failure by such mechanisms as excessive deflection, yielding under circumferential stress, and buckling failure.

### 2.1 Axial Forces in Buried Arches

Axial forces (ring compression forces or thrust) are a major consideration in the design of buried arches. The compressive strength of the arch material must be sufficient to withstand the axial forces in the structure with an adequate factor of safety against buckling or compression failure.

Dupas and Pecker proved that the stiffness of the structure and the backfill have little effect on the magnitude or the distribution of the axial force in the arch (4); i.e., changing the thickness of the arch has very little effect on the axial forces, and the relative stiffness of the structure and the backfill has no significant effect on axial forces, even for shallow cover conditions.

White and Layer have developed a simple procedure for calculating axial forces in culvert structures based on ring compression theory and have applied this method to the design of a number of culvert structures (11). This theory assumes that the culvert carries the weight of the backfill above the crown through pure ring compression action. The maximum axial force at the footing of an arch structure is

$$P = \frac{\gamma HS}{2 \cos \theta}$$

where

P = axial force, in kips per foot,

$\gamma$ = unit weight of backfill, in kips per cubic foot,

H = depth of cover over crown, in feet,

S = span, in feet, and

$\theta$ = angle between culvert wall and vertical at the footing.

The ring compression forces in arches can also be approximated from the following equation by finite element analysis with sufficient accuracy for use in design (2, 4):

$$P = K_{P1} S^2 + K_{P2} \gamma HS + K_{P3} L_L$$

where

$P$ = maximum axial (ring compression) force in the culvert, in kips per foot,

$K_{P1}$ = a coefficient for axial force due to backfill up to the crown,

$K_{P2}$ = a coefficient for axial force due to the cover over the crown,

$K_{P3}$ = a coefficient for axial force due to live load,

$\gamma$ = unit weight of backfill,

$H$ = the cover depth over the crown,

$S$ = the span, and

$L_L$ = the live load.

The values of $K_{P1}$ and $K_{P2}$ vary with the rise/span (R/S) ratio of the structure, and the value of $K_{P3}$ varies with the cover depth/span (H/S) ratio, as shown in the curves of Fig. 14 [developed by Duncan (4)].

Figure 15 shows a comparison between axial forces calculated using the equation of White and Layer and those calculated by means of finite element analysis (4). It may be seen that the axial forces calculated using finite element analysis are somewhat larger than those determined using the ring compression theory of White and Layer (1960).

The reasons for these differences are:

1. The finite element analysis method indicates that arches carry loads that exceed the weight of the fill directly over the structure. Thus 'negative arching' occurs (Fig. 1), and a portion of the weight of the fill

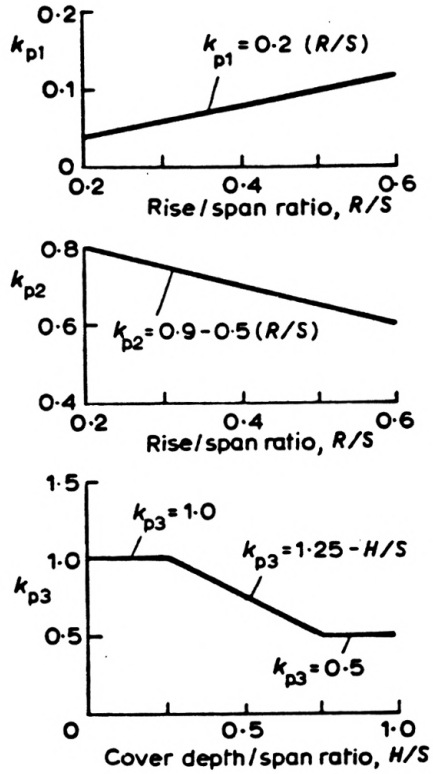


Fig. 14. Values of axial forces coefficients for arches (Duncan).

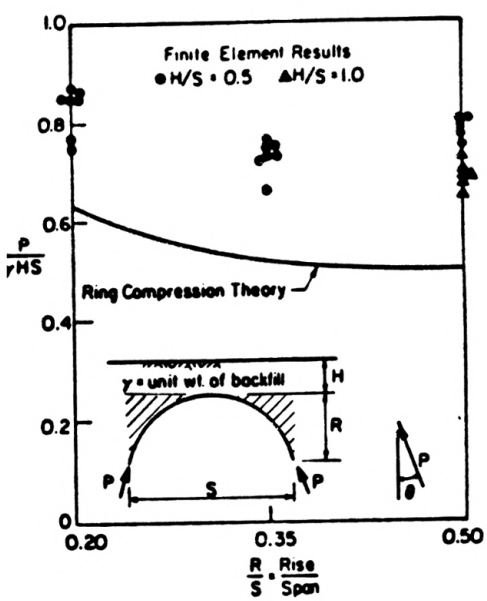


Fig. 15. Comparison of axial forces from ring compression theory and finite element analysis.

adjacent to the arch is carried by the structure, as well as the weight of the fill above the structure.

2. The finite element results include the weight of soil within the shaded area in Fig. 15, whereas they are neglected in the ring compression theory.

Although the Ring Compression Theory developed by White and Layer gives lower values of ring compression force than those determined from finite element analysis, it has provided a useful means of estimating axial forces for design, as shown by many successful applications.

## 2.2 Bending Moments in Buried Arches

Arch conduits must have sufficient flexural stiffness and bending moment capacity so that they maintain their shape and withstand nonuniform live loads under shallow covers. Therefore, it is of interest to examine the magnitudes and the distributions of moments in culvert structures, especially in the case of shallow cover over the crown.

Figure 16 shows an example of the variations in bending moments with fill height. The bending moments were calculated by the author (Appendix) for a semi-circular arch of 10 ft. radius using the virtual work method under two different heights of backfill, 2 ft. in Fig. 16.a and 10 ft. in Fig. 16.b. As backfill increases, the magnitude of the positive moment (downward flexure) at the crown of the arch increases and the

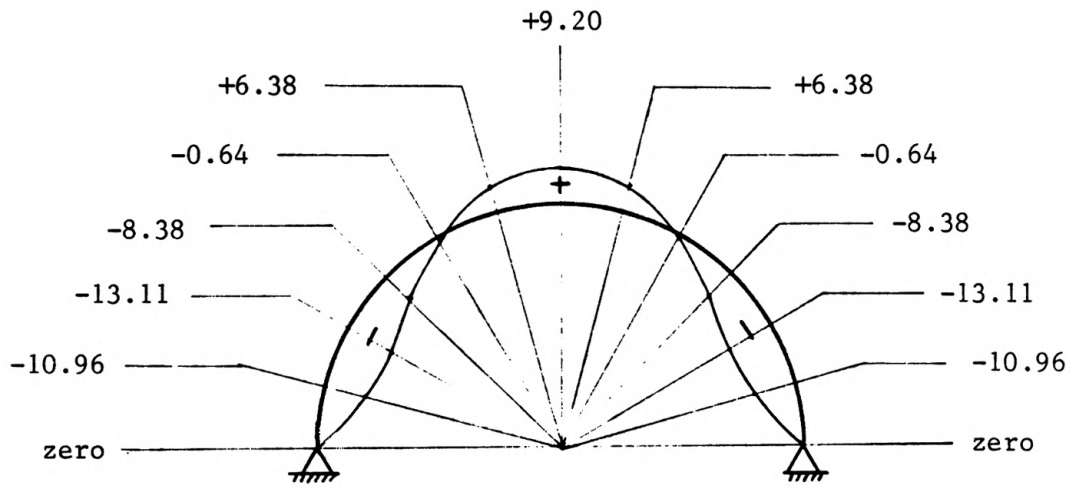


(a) Depth of fill = 2 ft. and live load HS20 truck wheel (Bending moment per linear foot, kip•ft.).

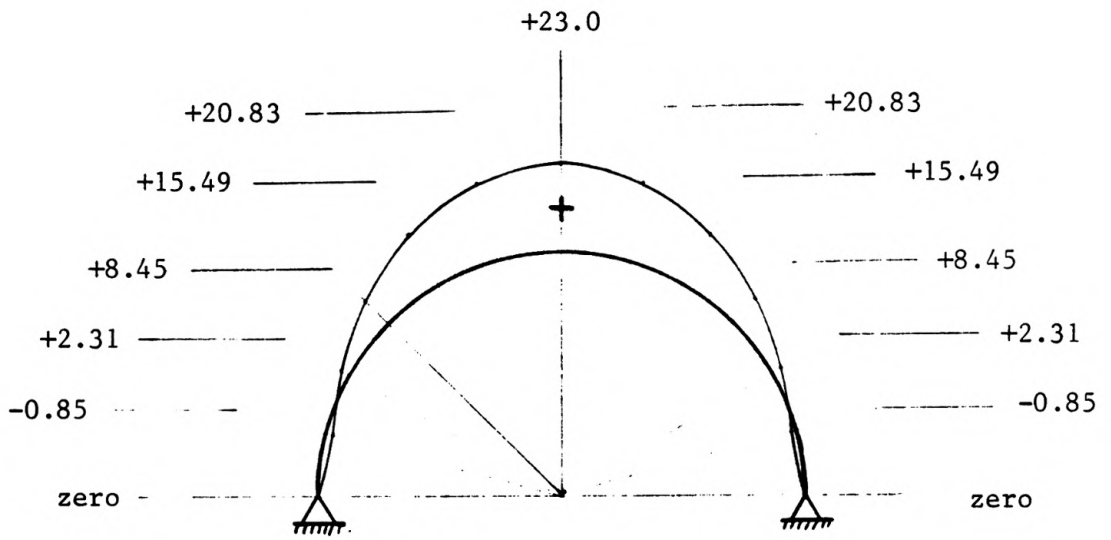


(b) Depth of fill = 10 ft. and live load HS20 truck wheel (Bending moment per linear foot, kip•ft.).

Fig. 16. Maximum bending moment diagrams calculated by the virtual work method due to backfill ($\gamma$ = 115 p.c.f., and $\phi$ = 32°) and live load AASHTO truck loading HS20-44.

negative moments (outward flexure) at the quarter points decrease and are reversed to positive moment under higher backfills.

Duncan studied the distributions of bending moments in identical arch structures with two different types of backfill, and found that the better quality backfill (a well-graded gravel compacted at 100% relative compaction as determined by the Standard AASHTO compaction test) induces smaller moments in the structure than the poorer quality backfill (a clay of low plasticity compacted to 95% relative compaction). Duncan also found that bending moments are larger in a stiffer arch than in a more flexible arch, both with the same backfill material. Therefore, an increase in backfill stiffness (all other factors being equal) results in a reduction in bending moments. Conversely, an increase in culvert stiffness (all other factors being equal) results in an increase in bending moments.

It has been found that bending moments calculated by finite element analysis may be related to the relative stiffness (or the relative flexibility) of the backfill and the culvert structure by means of a dimensionless ratio defined as follows (Nielson, 1972; Selig, 1972) (4):

$$N_f = \frac{E_s S^3}{EI}$$

where

$N_f$ = flexibility number,

$E_s$ = secant modulus of backfill soil, in kips per square foot,

S = span, in feet,

E = Young's modulus for the culvert, in kips per square foot, and

I = moment of inertia per foot of culvert, in feet$^4$ per foot.

Examination of the results of a large number of finite element analyses of arch culverts with various types of backfill indicates that the value of $E_s$ in the vicinity of the quarter point of the arch is approximately equal to the average value for the backfill. Duncan used this observation to develop the approximate relationships between $E_s$ and backfill depth for different soils that are shown in Fig. 17. These curves may be used to estimate the value of $E_s$ for a given type of backfill, degree of compaction, and depth of cover over the quarter point of a structure.

The maximum bending moment due to backfill loads, determined by finite element analysis, can be represented approximately by (2, 4):

$$M_B = R_B \, (K_{m1} \, \gamma S^3 - K_{m2} \, \gamma S^2 \, H)$$

where

$M_B$ = maximum bending moment in the culvert, in kip-feet per foot,

$K_{m1}$ and $K_{m2}$ are moment coefficients that vary with flexibility number, $N_f$, as shown in Fig. 18,

$R_B$ = the moment reduction factor for backfill moments, governed by the rise/span ratio, as shown in Fig. 19,

S = span,

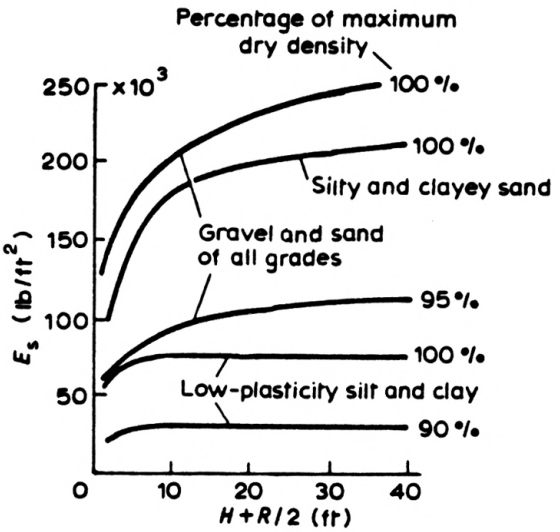


Fig. 17. Values of Secant Modulus of backfill $E_s$ used by Duncan.

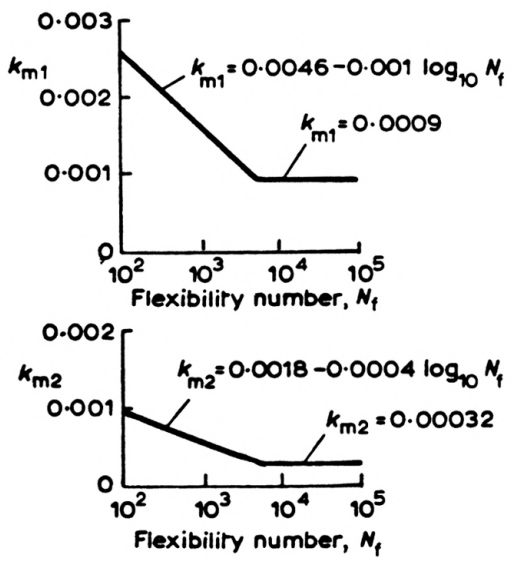


Fig. 18. Backfill moment coefficients for arches (Duncan).

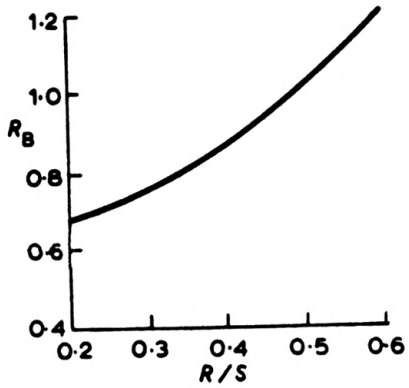


Fig. 19. Moment reduction factor for arches (Duncan).

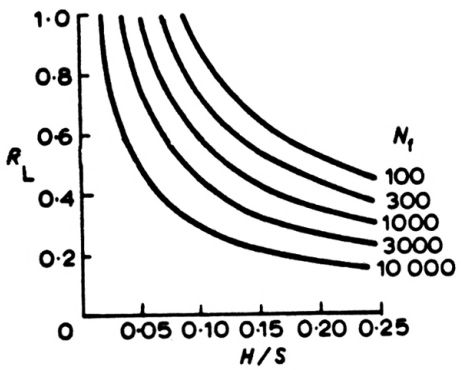


Fig. 20. Reduction factor for live-load moments on arches (Duncan).

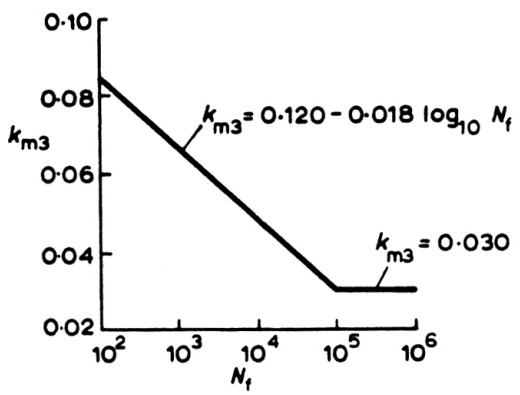


Fig. 21. Live-load moment coefficients for arches (Duncan).

H = depth of backfill over the arch crown, and

$\gamma$ = unit weight of backfill.

The finite element technique was also used to calculate bending moments due to live loads on the surface. Live loads over the crown cause downward flexure of the crown, and live loads over the quarter point cause inward flexure of the quarter point.

At shallow cover depths, where moments due to live loads are important, the moment due to backfill loads will be positive, indicating inward flexure at the quarter point due to backfill loads. Therefore, with the live load over the quarter point, the effects of the backfill and the live loads combine to produce a moment at the quarter point that is larger than the moment at any other position.

The additional moment at the quarter point due to highway loads may be calculated from the following empirical equation (4), which closely approximates the results of finite element analysis:

$$\Delta M_L = R_L \, K_{m3} \, S \, L_L$$

where

$\Delta M_L$ = additional moment at the quarter point due to live load, in kip-feet per foot, and

$R_L$ = reduction factor for live load moment, which varies with cover depth H, and flexibility number $N_f$, as shown in Fig. 20. $R_L$ also can be calculated using the formula

$$R_L = \frac{3.77 - 0.75 \log_{10} N_f}{(H/S)^{0.75}} \quad (R_L \leqslant 1.0).$$

$K_{m3}$ = live load moment coefficient, which varies with the flexibility number $N_f$, as shown in Fig. 21.

When a culvert is subjected to repeated traffic loadings, the surrounding backfill is loaded and unloaded repeatedly. As a result, the effective modulus of backfill, $E_s$, increases from the value for the first loading, given in Fig. 17, to a higher value for unloading and reloading. Although Fig. 17 underestimates the backfill modulus for repeated traffic loading, it is conservative and is considered suitable for design purposes.

## CONCLUSION

The vertical load transmitted from the embankment to the arch depends on the depth of back-fill materials and their characteristics as well as on the compressibility and the degree of compaction of the fill materials adjacent to the arch.

Lateral earth forces can be obtained (or calculated) satisfactorily as active lateral loads by Rankine's Theory.

Highway live loads transmitted to a buried arch depend on depth of fill, type of pavement and wheel load.

Axial forces in buried arches calculated by finite element analysis are larger than those calculated by Ring Compression Theory. However, the latter method has been sufficient for design purposes and has had many successful applications.

Bending moments calculated by virtual work method agreed with those calculated by finite element analysis.

## REFERENCES


1. Bowles, J. E., Foundation Analysis and Design, 3rd edition, McGraw-Hill Book Company, 1982.

2. Bulson, P. S., Buried Structures Static and Dynamic Strength, Chapman and Hall, 1985.

3. Concrete Construction, Concrete Construction Publications, INc., April 1988, Vol. 33, No. 4.

4. Duncan, J. M., "Behavior and Design of Long-Span Metal Culverts," Journal of the Geotechnical Engineering Division, ASCE No. GT3, March 1979, pp. 399-418.

5. Hydraulic Structures Reference Series, "Concrete Culverts and Conduits," Portland Cement Association, 1975.

6. Lambe, T. W., William, T., Soil Mechanics, John Wiley and Sons, 1969.

7. Marston, A., Anderson, A. O., "The Theory of Loads on Pipes in Ditches and Tests of Cement and Clay Drain Tile and Sewer Pipe," Iowa Engineering Experiment Station Bulletin.

8. Scott, R. E., Schoustra, J. J., Soil Mechanics and Engineering, McGraw-Hill Book Company, 1968.

9. Selig, E. T., Abel, J. F., Kulhaway, F. H., "Long-Span Buried Structure Design and Construction," Journal of the Geotechnical Engineering Division, ASCE No. GT7, July 1978.

10. Spangler, M. G., "Analysis of Loads and Supporting Strengths and Principles of Design for Highway Culverts," HRB Proceedings, 26th Annual Meeting, 1966.

11. White, H. L., Layer, J. P., "The Corrugated Metal Conduits as a Compression Ring," Proceedings, Highway Research Board, Vol. 39, 1960.

12. Wu, T. H., Soil Mechanics, 2nd Edition, Allyn and Bacon, Inc., 1976.

## ACKNOWLEDGMENTS

The author expresses his sincere gratitude to those persons whose guidance and assistance made this report possible:

Dr. Robert R. Snell, Head of the Civil Engineering Department, who made his graduate study possible here at Kansas State University.

Professor Wayne W. Williams, his major advisor, for his most helpful advice and guidance.

Dr. Cecil H. Best, a member of his committee, who reviewed the entire manuscript critically and made several valuable suggestions.

Dr. John C. Matthews, for serving on his committee.

Mrs. Peggy Selvidge, for her patient and careful typing of this report.

# APPENDIX

Calculation of Bending Moments Using the Virtual Work Method for a Semi-circular Arch of 10 ft. Radius Under Two Different Heights of Backfill.

1. Arch Buried Under 2.0 ft. of Backfill on Top of its Crown.

Assumptions:

$\gamma$ (for soil) = 115.0 pcf.

$\gamma$ (for reinforced concrete) = 155.0 pcf.

$\emptyset = 32^{o}$; $K_a = 0.30$.

Live load = AASHTO truck loading HS20-44.

Thickness of reinforced concrete arch = 10.0 in.

(a) Bending Moments Due to Vertical Loads (Figs. A-1, 2 & 3):

$W_{D.L.} \cong$ uniformly distributed load due to soil load + own weight

$$= 115.0 \times 2.0 + 155.0 \times \frac{10}{12} .$$

$W_{D.L.} = 359.17$ psf.

$\simeq 0.360$ ksf.

$$W_{L.L.} = \frac{16{,}000}{(1.75 \times 2)^2} = 1306 \text{ psf.}$$

$W_{L.L.} = 1.306$ ksf.

$W_T = W_{D.L.} + W_{L.L.}$

$= 0.360 + 1.306$

$= 1.666$ ksf.

Since the arch cross section is constant, therefore consider EI constant for all sections of the arch.

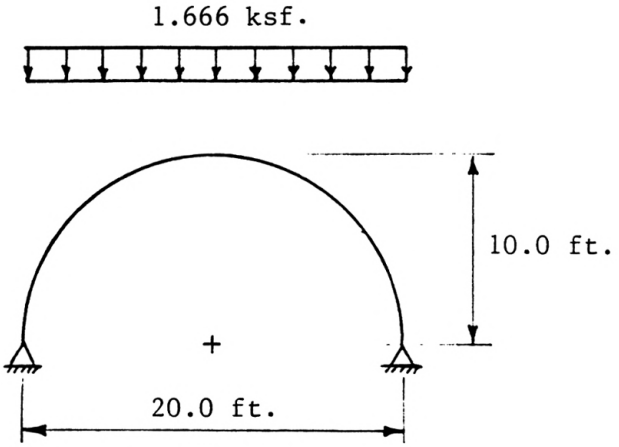


(a) Crown loading

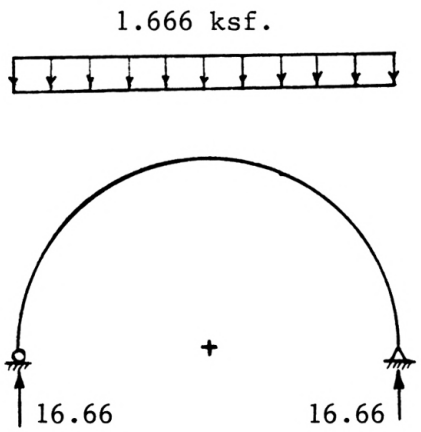


(b) Main system
Loading "0"

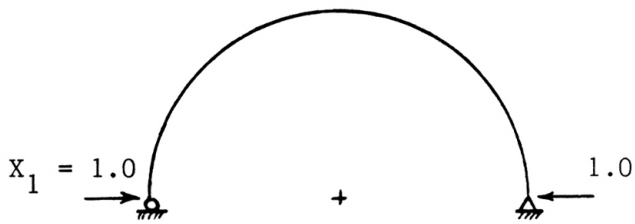


(d) Loading "1"

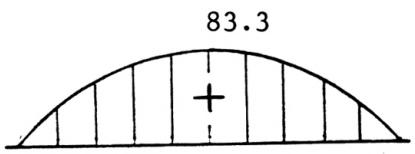


(c) $M_0$-diagram

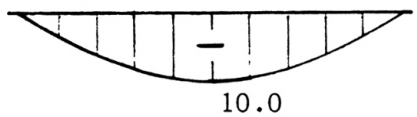


(e) $M_1$-diagram

Fig. A-1. Bending moments analysis due to vertical loads.

| | X | Y |
|---|---|---|
| 1 | 0.341 | 2.588 |
| 2 | 1.340 | 5.00 |
| 3 | 2.929 | 7.071 |
| 4 | 5.000 | 8.660 |
| 5 | 7.412 | 9.659 |
| 6 | 10.00 | 10.00 |

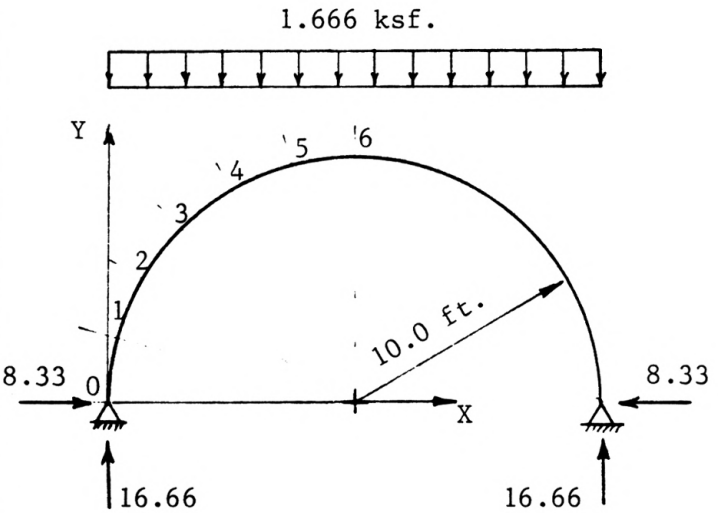


Fig. A-2. Reactions due to vertical loads.

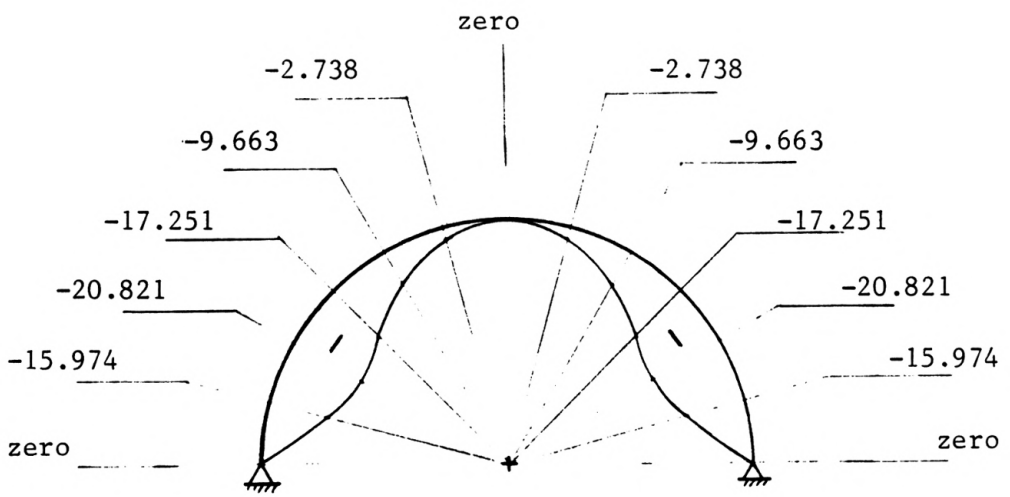


Fig. A-3. Bending moment diagram due to vertical loads.

Deformations:

$$EI\ \delta_{10} = \int M_1 M_0\ dL$$

$$= \frac{-4}{5}\left(\frac{2}{3} \times 83.3 \times 20.0\right) \times 10.0.$$

$$EI\ \delta_{10} = -8885.33$$

$$EI\ \delta_{11} = \int M_1 M_1\ dL$$

$$= \frac{+4}{5}\left(\frac{2}{3} \times 10.0 \times 20.0\right) \times 10.0.$$

$$EI\ \delta_{11} = +1066.67.$$

Displacement conditions:

at A: $\delta_1 = 0.$

$$\delta_{10} + X_1\delta_{11} = 0.$$

$$X_1 = \frac{-\delta_{10}}{\delta_{11}} = \frac{-(-8885.33)}{1066.67}.$$

$$X_1 = 8.33 \text{ kips.}$$

(b) Bending Moments Due to Lateral Earth Pressure (Fig. 4-A):

$$e = \gamma h\ K_a.$$

$e_6 = 115.0 \times 2.0 \times 0.30 = 69.0$ psf. $= 0.069$ ksf.

$e_0 = 115.0 \times 12.0 \times 0.30 = 414.0$ psf. $= 0.414$ ksf.

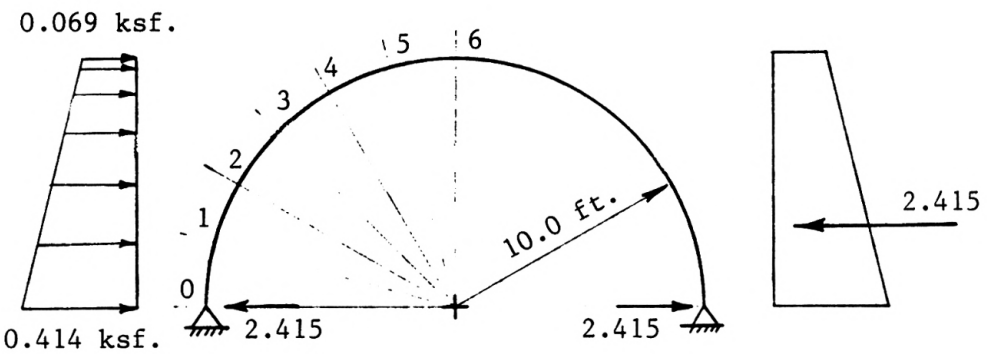


(a) Lateral earth pressure on the arch.

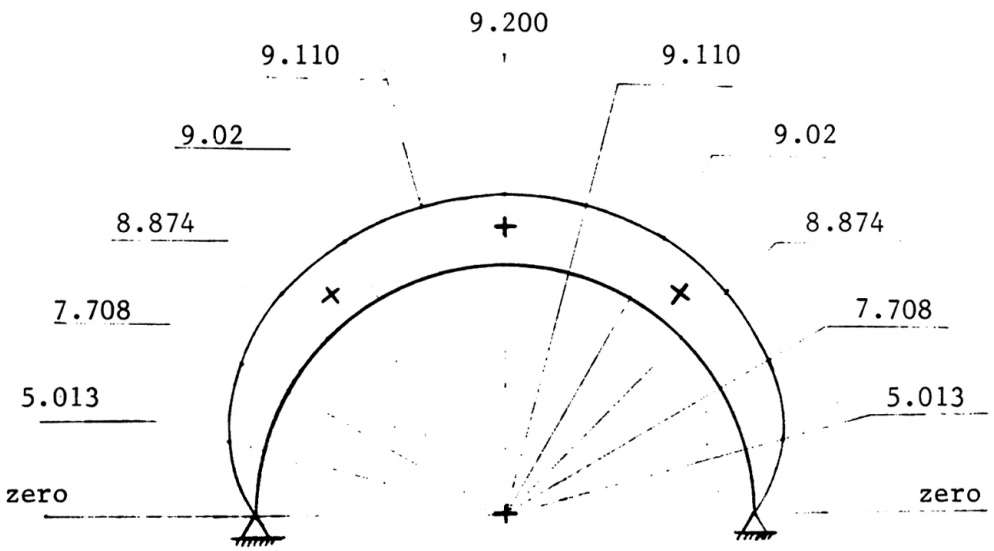


(b) Bending moment diagram due to lateral earth pressure

Fig. A-4. Bending moments analysis due to lateral earth pressure.

| Point | e (ksf.) | h (ft.) | P (k/ft.) |
|---|---|---|---|
| 0 | 0.414 | | |
| | | 2.588 | 0.956 |
| 1 | 0.325 | | |
| | | 2.412 | 0.683 |
| 2 | 0.241 | | |
| | | 2.071 | 0.426 |
| 3 | 0.170 | | |
| | | 1.589 | 0.226 |
| 4 | 0.115 | | |
| | | 1.00 | 0.098 |
| 5 | 0.081 | | |
| | | 0.341 | 0.026 |
| 6 | 0.069 | | |

Figure A-5 shows the final reactions and the final bending moments due to vertical and horizontal loads.

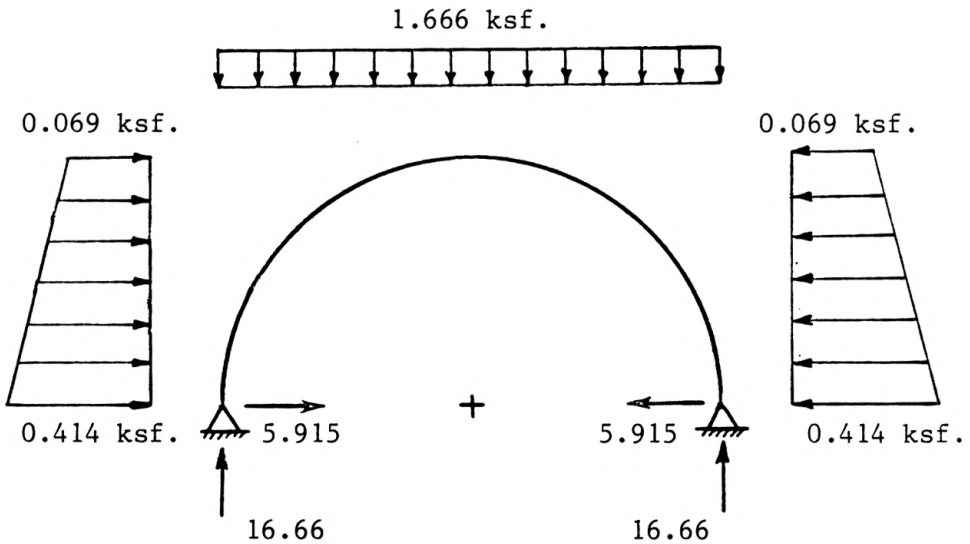


(a) Vertical and horizontal loads and final reactions.

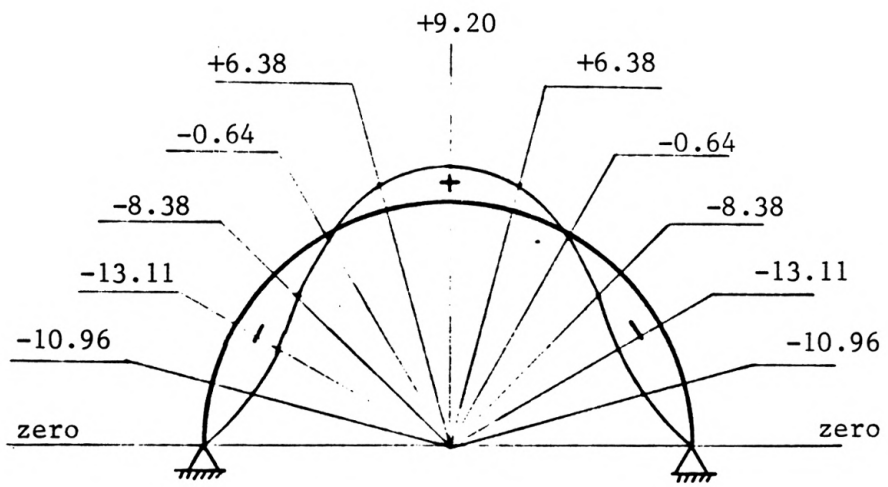


(b) Final bending moment diagram B.M.D. obtained by adding B.M.D. due to vertical forces to B.M.D. due to horizontal forces.

Fig. A-5. Final reactions and final bending moments.

2. Arch Buried Under 10.0 ft. of Backfill on Top of its Crown.

Assumptions:

$\gamma$ (for soil) = 115.0 pcf.

$\gamma$ (for reinforced concrete) = 155.0 pcf.

$\emptyset = 32^{o}$; $K_a = 0.30$.

Live load = AASHTO truck loading HS20-44.

Thickness of reinforced concrete arch = 10.0 in.

(a) Bending Moments Due to Vertical Loads (Figs. A-6, 7 & 8):

$W_{D.L.} \cong$ uniformly distributed load due to soil load + own weight

$$= 115.0 \times 10.0 + 155.0 \times \frac{10}{12}$$

$W_{D.L.} = 1279.17$ psf.

$\simeq 1.28$ ksf.

$$W_{L.L.} = \frac{4 \times 16{,}000}{(17.5 \times 33.5)} = 109.17 \text{ psf.}$$

$W_{L.L.} = 0.11$ ksf.

$W_T = W_{D.L.} + W_{L.L.}$

$= 1.28 + 0.11$

$= 1.39$ ksf.

Since the arch cross section is constant, therefore consider EI constant for all sections of the arch.

Deformations:

$$EI\ \delta_{10} = \int M_1 M_0\ dL$$

$$= \frac{-4}{5} \left(\frac{2}{3} \times 69.5 \times 20.0\right) \times 10.0.$$

$EI\ \delta_{10} = -7413\ 33$

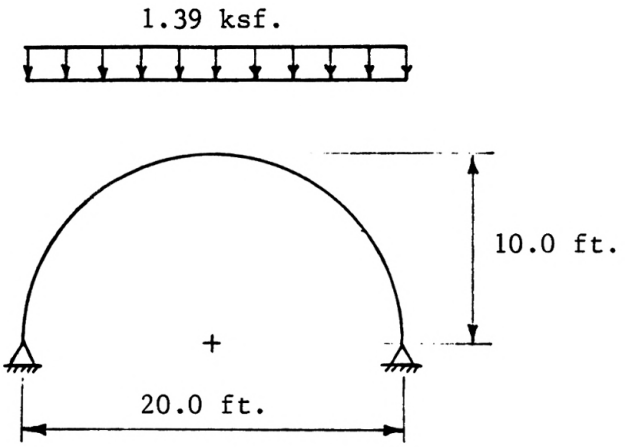


(a) Crown loading.

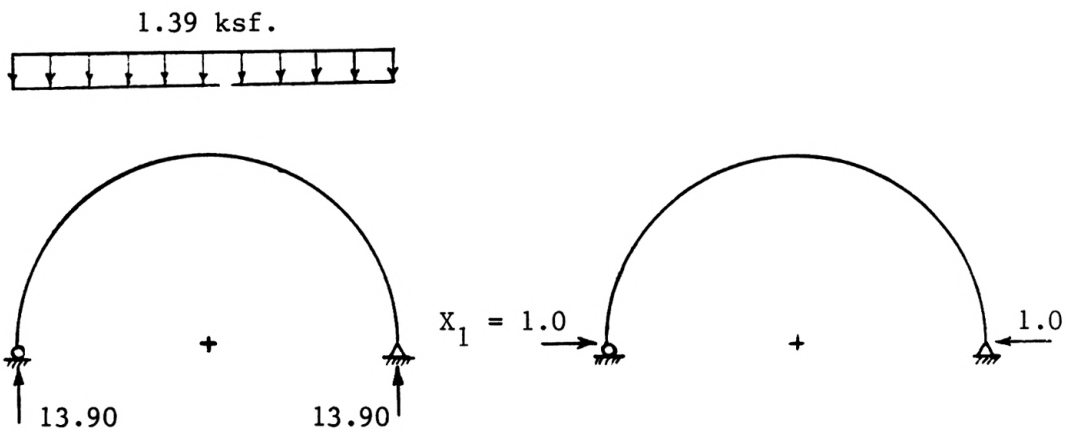


(b) Main system loading "0"

(d) Loading "1"

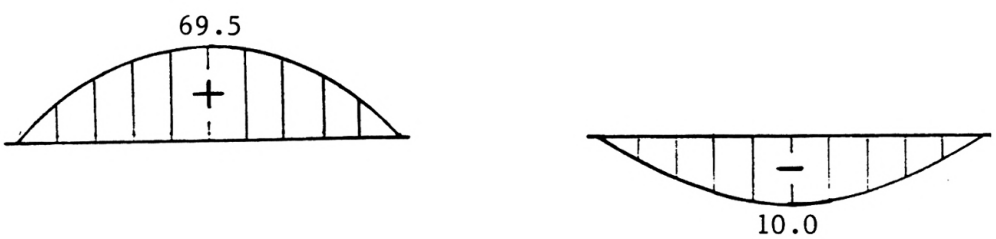


(c) $M_0$-diagram

(e) $M_1$-diagram

Fig. A-6. Bending moments analysis due to vertical loads.

| | X | Y |
|---|---|---|
| 1 | 0.341 | 2.588 |
| 2 | 1.340 | 5.00 |
| 3 | 2.929 | 7.071 |
| 4 | 5.00 | 8.660 |
| 5 | 7.412 | 9.659 |
| 6 | 10.00 | 10.00 |

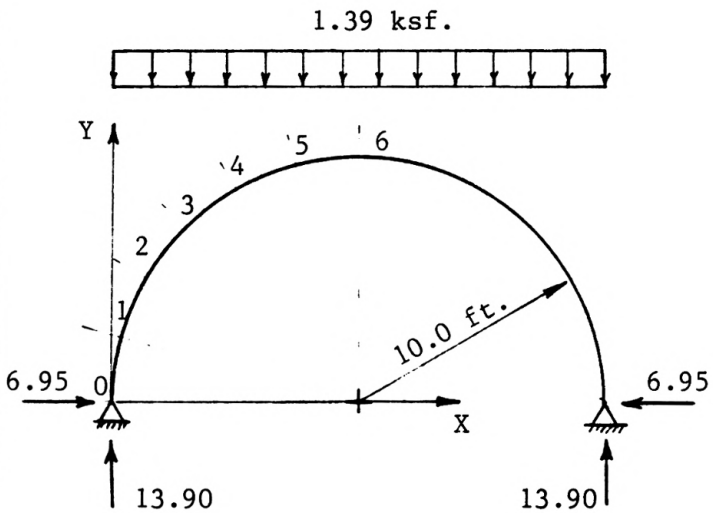


Fig. A-7. Reactions due to vertical loads.

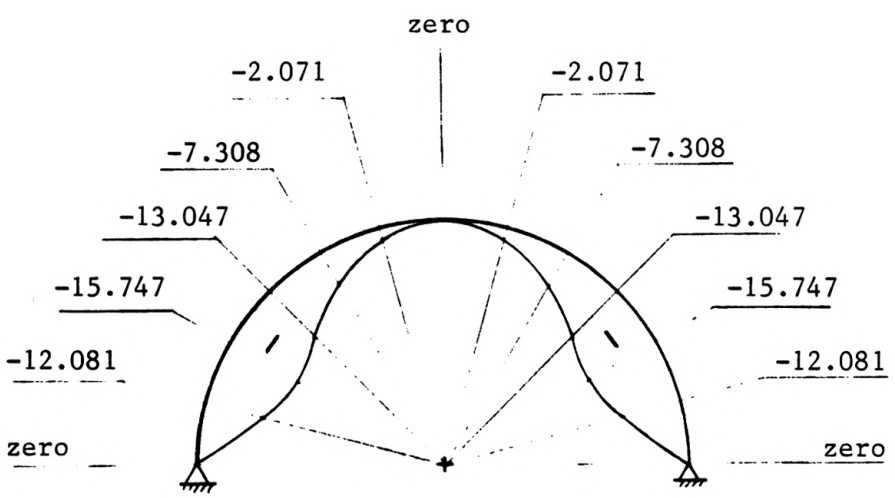


Fig. A-8. Bending moment diagram due to vertical loads.

$$EI\ \delta_{11} = \int M_1 M_1\ dL$$

$$= \frac{4}{5}\left(\frac{2}{3} \times 10.0 \times 20.0\right) \times 10.0.$$

$$EI\ \delta_{11} = +1066.67.$$

Displacement conditions:

at A: $\delta_1 = 0.$

$$\delta_{10} + X_1\ \delta_{11} = 0.$$

$$X_1 = \frac{\delta_{10}}{\delta_{11}} = \frac{-(-7413.33)}{1066.67}$$

$$X_1 = 6.95 \text{ kips.}$$

(b) Bending Moments Due to Lateral Earth Pressure (Fig. 9-A):

$$e = \gamma h\ K_a.$$

$e_6 = 115.0 \times 10.0 \times 0.30 = 345.0$ psf. $= 0.345$ ksf.

$e_0 = 115.0 \times 20.0 \times 0.30 = 690.0$ psf. $= 0.690$ ksf.

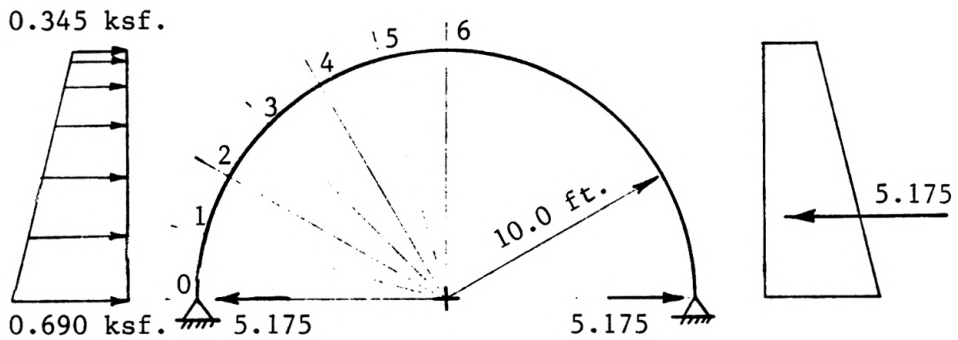


(a) Lateral earth pressure on the arch.

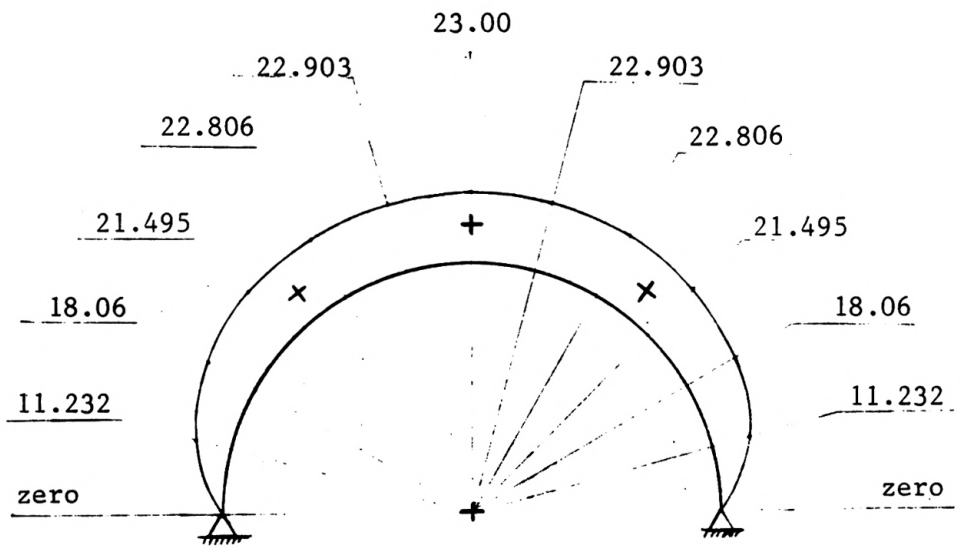


(b) Bending Moment Diagram due to lateral earth pressure.

Fig. A-9. Bending moments analysis due to lateral earth pressure.

| Point | e (ksf.) | h (ft.) | P (k/ft.) |
|---|---|---|---|
| 0 | 0.690 | | |
| | | 2.588 | 1.670 |
| 1 | 0.601 | | |
| | | 2.412 | 1.348 |
| 2 | 0.518 | | |
| | | 2.071 | 0.997 |
| 3 | 0.446 | | |
| | | 1.589 | 0.670 |
| 4 | 0.391 | | |
| | | 1.00 | 0.373 |
| 5 | 0.356 | | |
| | | 0.341 | 0.117 |
| 6 | 0.345 | | |

Figure A-10 shows the final reactions and the final bending moments due to vertical and horizontal loads.

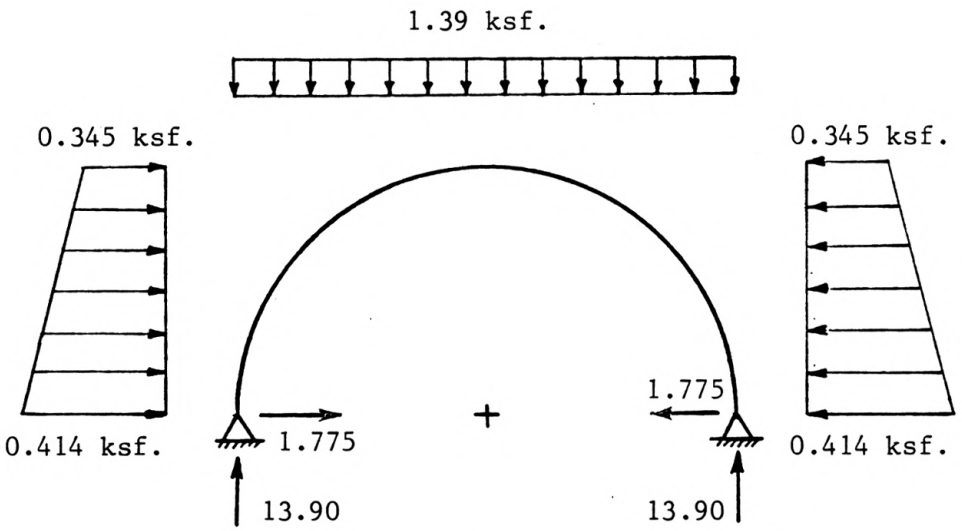


Vertical and horizontal loads and final reactions.

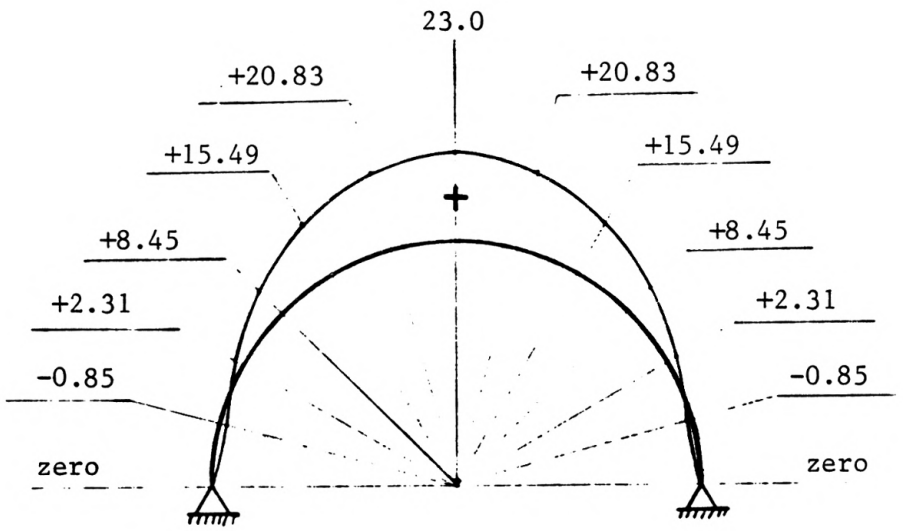


Final bending moment diagram B.M.D. obtained by adding B.M.D. due to vertical forces to B.M.D. due to horizontal forces.

Fig. A-10. Final reactions and final bending moments.

# METHODS OF ESTIMATING FORCES IN BURIED ARCHES

by

MOUNIR G. EL-AASAR

B.S., Alexandria University,
Alexandria, Egypt,
1983

- - - - - - - - - - - - - - - - - - - - - - -

AN ABSTRACT OF A MASTER'S REPORT

submitted in partial fulfillment of the

requirements for the degree

MASTER OF SCIENCE

Department of Civil Engineering

KANSAS STATE UNIVERSITY
Manhattan, Kansas

1988

## ABSTRACT

Buried arches are subjected to embankment and wheel loads. Vertical loads from embankments depend on the settlement of the fill adjacent to the conduit relative to the fill directly over it, as shown by Marston's theory. Methods for calculating vertical earth loads, lateral earth loads and highway live loads are presented in this report. These calculations show that vertical load can be assumed to be distributed uniformly over the top of the arch, that lateral earth loads can be considered to be active lateral loads acting over the vertical projection, and that wheel loads are distributed over large subgrade areas when rigid pavements are used, while flexible pavements do not provide wide live load distribution.

Thrust and bending moment are the two main internal effects that govern the design of a buried arch. Axial forces can be calculated by using ring compression theory or the finite element method. The comparison between the results obtained from these two methods shows that values obtained by finite element are somewhat larger. Bending moments calculated by using the virtual work method presented by the author show good agreement with the results obtained by finite element analysis. Approximate equations for calculating axial forces and bending moments by finite element methods are presented.